Apoptosis 2005; **10**: 997–1007

Caspase-independent death of Leber's hereditary optic neuropathy cybrids is driven by energetic failure and mediated by AIF and Endonuclease G

C. Zanna, A. Ghelli, A. M. Porcelli, A. Martinuzzi, V. Carelli and M. Rugolo

Dipartimento di Biologia Ev. Sperimentale, Università di Bologna, Bologna 40126, Italy (C. Zanna, A. Ghelli, A. M. Porcelli, M. Rugolo); IRCCS "E.Medea" , Conegliano, Treviso 31015, Italy (A. Martinuzzi); Dipartimento di Scienze Neurologiche, Università di Bologna, Bologna 40123, Italy (V. Carelli)

Leber's hereditary optic neuropathy (LHON) is associated with mitochondrial DNA point mutations affecting different subunits of complex I. By replacing glucose with galactose in the medium, cybrids harboring each of the three LHON pathogenic mutations (11778/ND4, 3460/ND1, 14484/ND6) suffered a profound ATP depletion over a few hours and underwent apoptotic cell death, which was caspase-independent. Control cybrids were unaffected. In addition to cytochrome c, apoptosis inducing factor (AIF) and endonuclease G (EndoG) were also released from the mitochondria into the cytosol in LHON cybrids, but not in control cells. Exposure of isolated nuclei to cytosolic fractions from LHON cybrids maintained in galactose medium caused nuclear fragmentation, which was strongly reduced by immuno-depletion with anti-AIF and anti-EndoG antibodies. In conclusion, the caspase-independent death of LHON cybrids incubated in galactose medium is triggered by rapid ATP depletion and mediated by AIF and EndoG.

Keywords: ATP; complex I; cybrid cells; glucose deprivation; LHON

Introduction

Leber's hereditary optic neuropathy (LHON) is a genetically determined degeneration of retinal ganglion cells (RGC) leading to acute or subacute loss of central vision.[1,2] The primary pathogenic defect resides in mitochondrial DNA (mtDNA), the three point mutations at nucleotide positions 11778/ND4, 3460/ND1 and 14484/ND6 being the most frequent in patients worldwide. These mutations affect different subunits of complex I, the first site of the respiratory chain. It still remains unclear how the aminoacid substitutions caused by LHON mutations, which induce only subtle changes in complex I electron-transport function, lead to RGC death.[3]

Histopathological studies of optic nerve specimens from LHON patients have shown a dramatic loss of axons with no evidence for inflammatory events but with still ongoing low-grade degeneration.[4] This suggests that neurodegeneration might result from a synchronized wave of apoptotic cell death that propagates through RGC. Absence of inflammatory features is also indicated by the lack of response to steroid-based therapies and the absence of blood-nerve barrier damage revealed by fluorangiography, which fails to show fluorescein leakage.[1,2] The "apoptotic" hypothesis for RGC death has recently received support from studies on transmitochondrial hybrids or cybrids. Cybrids are one of the few cell models available to investigate LHON in the absence of an animal model of this disease and given the inability to study RGC directly.

The cybrid model is based on the repopulation of an immortalized, usually cancer derived, cell line previously devoid of its original mtDNA with patient-derived mutant mitochondria.[5] Recent studies have shown that osteosarcoma-derived LHON cybrids were more prone to Fas-induced apoptotic death than control cybrids.[6] Similar results were also obtained by growing LHON cybrids in glucose-free galactose-supplemented medium. This is a very well established method to reveal an oxidative phosphorylation dysfunction by forcing the cells to rely on mitochondrial respiratory chain to synthesize ATP.[7] We recently reported that incubation in galactose medium caused apoptotic death of LHON cybrids, but not of 143B parental cell line or control cybrids.[8] Apoptosis was recognized by some typical hallmarks, such as changes in nuclear morphology, chromatin condensation and fragmentation of chromosomal DNA, and release of cytochrome c into the cytosol, clearly indicating a mitochondria-dependent cell death pathway.[8] However, despite the release of cytochrome c, no activation of

Correspondence to: A. Ghelli, Dipartimento di Biologia Evoluzionistica Sperimentale, Universita' di Bologna, Via Irnerio 42, 40126 Bologna, Italy. Tel.: +39 051 2091306; Fax: +39 051 242576; e-mail ghelli@alma.unibo.it

caspase-3 could be determined by means of western blot analysis in LHON cybrids incubated in galactose.[9]

In the classical apoptotic process, cytochrome c release into the cytoplasm drives the assembly of the apoptosome, which in turn triggers activation of caspase-9 and downstream executioner caspases.[10,11] A key event in this pathway is the caspase-3-mediated cleavage of DFF45 (DNA fragmentation factor 45 kDa)/ICAD (inhibitor of caspase-activated deoxyribonuclease DFF40/CAD) in humans and mice, respectively. DFF45 cleavage causes DFF40 release and entry into the nucleus, followed by both chromatin condensation and internucleosomal DNA fragmentation.[12,13]

Although caspase-mediated apoptosis is the principal form of cell death, much evidence now shows that caspase-independent pathways are just as important,[14] namely the mechanism mediated by apoptosis inducing factor (AIF) and endonuclease G (EndoG), two mitochondrial apoptogenic factors. AIF is a flavoprotein exhibiting NADH oxidase activity, normally present in the mitochondrial intermembrane space[15] or loosely associated with the inner membrane.[16] Recently it has been shown that AIF is also required for the assembly and maintenance of complex I.[17] In response to apoptotic stimuli, AIF is released into the cytosol and translocates into the nucleus where it induces chromatin condensation and large-scale DNA fragmentation.[15,18] EndoG, like AIF, has been shown to redistribute from the mitochondria to the nucleus, where it causes oligonucleosomal DNA fragmentation.[19] Subsequent studies demonstrated that EndoG catalyzes both high molecular weight DNA cleavage and oligonucleosomal DNA breakdown in a sequential fashion, and cooperates with DNAse I and exonuclease to facilitate DNA processing.[20] In *Caenorhabditis elegans,* AIF has been shown to interact with EndoG, both in genetic and in biochemical terms. *In vitro*, recombinant *C. elegans* AIF and EndoG synergize to mediate DNA degradation.[21] However, in mammalian cells these factors can induce chromatin breakdown independent of one another.[18,19]

The major impact on the pathophysiology of LHON is likely to involve an energetic deficit. This is suggested by the reduced rate of ATP synthesis dependent on complex I substrates observed in digitonin-permeabilized cybrids with the 11778/ND4 LHON mutation, which was specifically rescued by allotopic expression of ND4 subunit.[22] Reduction of *in vitro* mitochondrial ATP synthesis is now being reported also in cybrids with the 3460/ND1 and 14484/ND6 LHON mutations.[23] The inability of LHON cybrids to maintain ATP levels during incubation in galactose medium also indirectly supports this hypothesis.[9] The aim of the present study was to evaluate whether the energetic failure occurring in galactose medium could influence the pathway of cell death. The time-course of ATP content of control and LHON cybrids bearing the pathogenic mutations 11778/ND4, 14484/ND6, and 3460/ND1 (two different clones for each mutation), during incubation in galactose medium was determined. Furthermore, given that apoptotic cell death of LHON cybrids was characterized by oligonucleosomal DNA fragmentation[8] and that caspase-3 was not activated, we focused on the possible involvement of the other mitochondrial apoptogenic factors AIF and EndoG.

Materials and methods

Materials

MTT (3-[4,5-dimethylthiazol-2-yl]-2,5-diphenyltetrazoliumbromid), ATP, staurosporine and protease inhibitors cocktail were purchased from Sigma (Milan, Italy). Ac-DEVD-AMC, Hoechst-33342 and z-VAD-fmk were from Calbiochem (La Jolla, CA, USA). Antibodies used for western blot were as follows: anti-caspase-3, anti-actin, anti-cytochrome c, anti-AIF and secondary antibodies from Santa Cruz Biotechnology (Santa Cruz, CA, USA), anti-mtHSP70 from Transduction Laboratories (Lexington, KY, USA), anti-tubulin from Sigma (Milan, Italy), anti-DFF45 and anti-EndoG were from Prosci (Poway, CA, USA). ATP monitoring kit was from BioOrbit (Turku, Finland). Antibodies used for immunofluorescence were as follows: anti-cytochrome c (BD Bioscience Pharmingen, Milan, Italy), anti-AIF and anti-EndoG were the same used for western blot. Secondary fluorescent antibodies were from Jackson ImmunoResearch Lab. Inc. (Baltimore, PA, USA).

Cell lines and culture conditions

The parental human osteosarcoma cells (143B), control (HGA) and LHON cybrid cell lines used were the same as in our previous study.[8] Cells were grown in DMEM medium supplemented with 10% foetal calf serum (FCS, South America source from Gibco, Invitrogen, Italy), 2 mM L-glutamine, 100 U/ml penicillin, 100 μg/ml streptomycin and 0.1mg/ml bromodeoxyuridine. For the experiments, cells were seeded 4×10^4 cells/cm^2 and incubated in DMEM glucose-free medium supplemented with 5 mM galactose, 5 mM Na-pyruvate and 5% FCS (galactose medium) at 37°C in an incubator with a humidified atmosphere of 5% CO_2.

ATP measurement

The amount of cellular ATP was determined by using the luciferin/luciferase assay. Cells (3×10^5) were seeded in 6 well plates, incubated in DMEM-glucose or in DMEM-galactose medium. At the times indicated, cells were

scraped off the plate, harvested in PBS and protein content determined.[24] An aliquot was incubated with 5% perchloric acid for 1 min at 4°C and subsequently neutralised with 0.09 M Tris and 0.14 M K_2CO_3. After centrifugation at 10000 × *g* for 1 min, ATP content in the supernatant was measured in duplicate using the BioOrbit ATP monitoring kit, according to manufacturer's instructions, using an appropriate internal ATP standard for calibration.

Cell viability measurement

The percentage of viable cells was measured with the colorimetric 3-(4,5-dimethyl thiazol-2yl)-2,5-diphenyl tetrazolium bromide (MTT) assay, as previously described.[8]

Caspase-3 and DFF45 assays

Activated caspase-3 can cleave the oligopeptide substrate Ac-DEVD-AMC, therefore DEVDase activity was determined in cell lysates (100 μg) by fluorescence measurement as previously described.[25] Cleavage of caspase-3 was also directly assessed by Western blot, as described in ref.[26] DFF45 cleavage was detected with anti-DFF45 antibody (1:1000). Anti-tubulin antibody (1:500) was used as a control for loading. Primary antibodies were visualized using horseradish peroxidase-conjugated secondary antibodies diluted 1:2000. The chemiluminescence signals were revealed using an ECL western blotting kit (Amersham Bioscience, Buckinghamshire, UK) and measured with the Fluo-2 MAX Multimager system (Bio-Rad, Hertfordshire, UK).

Subcellular fractionation

After incubation in DMEM glucose- or galactose-medium, cells were harvested from five 75 cm^2 flasks, resuspended in 0.5 ml of 200 mM mannitol, 70 mM sucrose, 1 mM EGTA, 10 mM Hepes (pH 7.6), 100 μl/ml of protease inhibitors cocktail and homogenised for 30 strokes with a Dounce homogenizer. This and the subsequent steps were carried out at 4°C. Samples were centrifuged for 10 min at 500 × *g* and the resulting supernatant was centrifuged 20 min at 10,000 × *g*. The supernatant (cytosolic fraction) was stored at −80°C. The pellet (mitochondria-enriched fraction) was resuspended in 50 μl of PBS containing 1% Triton-X100, 0.5 mM EDTA, 0.6 mM PMSF and 100 μl/ml of protease inhibitors cocktail and stored at −80°C. Proteins (50–80 μg) were separated by 15% SDS PAGE and transferred onto a nitrocellulose membrane (Bio-Rad, Hertfordshire, UK). The membrane was treated with 5% non-fat milk in TBS-Tween 0.05% for 1 h and incubated with the anti-cytochrome c (1:500) anti-AIF (1:1000) and anti-EndoG (1:500) for 1 h at room temperature. Anti-HSP70 and anti-actin antibodies were diluted 1:1000. Antigen-antibody complexes were detected as above.

Immunofluorescence

Cells grown in 36 mm diameter wells were treated as indicated, fixed with 3.7% paraformaldehyde and permeabilized 10 min with 0.15% TritonX-100 at room temperature. Cells, blocked with 0.5% BSA, were probed with primary antibodies overnight at 4°C. Anti-cytochrome c and anti-EndoG antibodies were diluted 1:200. Then cells were washed with PBS and stained with secondary fluorescent goat-anti-mouse and goat-anti-rabbit antibodies. Fluorescence was visualized with a digital imaging system using an inverted epifluorescence microscope (Nikon Eclipse 300) and Omega Filter pinkel Set XF66-1 triband (Omega Optical Inc., Brattleboro, VT, USA). Images were captured with a back-illuminated CCD camera (Princeton Instruments, Trenton, NJ, USA) and acquisition/analysis software Metamorph (Universal Imaging Corp., Downingtown, PA, USA).

Cell-free system for nuclear fragmentation

Nuclei preparations, cytosolic extracts and apoptosis cell-free system were performed as described in ref.[27] with minor modifications. HeLa cells (25×10^6) were harvested, washed in PBS, resuspended in 10 volumes of nuclear buffer (NB, containing 10 mM Pipes, pH 7.4, 10 mM KCl, 2 mM $MgCl_2$, 1 mM DTT, 10 μM cytochalasin B and 1 mM PMSF) and transferred to a Dounce homogenizer for 10 min in ice. Cells were then gently lysed with 20 strokes of the pestle, layered over 30% (w/v) sucrose in NB and centrifugated at 800 × *g* for 10 min. Nuclear pellet was washed in NB and resuspended (2×10^7 nuclei/ml) in 10 mM Pipes pH 7.4, 80 mM KCl, 20 mM NaCl, 250 mM sucrose, 5 mM EGTA, 1 mM DTT, 1 mM PMSF, 50% glycerol and stored at −80°C.

Cytosolic extracts were obtained from 25×10^6 LHON cybrids grown in glucose medium or incubated in galactose medium (24 h). Cells were harvested, washed and resuspended in 0.5 ml of 50 mM Pipes, pH 7.4, 50 mM KCl, 5 mM EGTA, 2 mM $MgCl_2$, 1 mM DTT, 10 μM cytocalasin B, 1 mM PMSF, and transferred to a Dounce homogenizer for 10 min in ice. Cybrids incubated in galactose medium, after addition of 50 μM z-VAD-fmk, were gently homogenized with 40 strokes of the pestle, diluted 1:2 with 10 mM Hepes, 50 mM NaCl, 2 mM $MgCl_2$, 5 mM EGTA, 1 mM DTT, 2 mM

ATP, 10 mM phosphocreatine, 50 μg/ml creatine kinase, and centrifuged at 4°C for 10 min at 14000 $\times$ g. Supernatants from control and galactose-treated cells were concentrated in centricon YM-10 (Millipore, Bedford, MA, USA) at 4000 $\times$ g for 2 h at 4°C. Immunodepletion of AIF and EndoG was carried out in an aliquot of the supernatant obtained from cells incubated in galactose medium, by incubation with anti-AIF and anti-endoG antibodies (1:200) for 2 h at 4°C. Immunodepleted supernatant was then concentrated as above. Concentrated supernatants (about 30 μl) were incubated with 1×10^5 HeLa nuclei overnight at 37°C, then loaded with 1 μg/ml Hoechst for 30 min at 37°C. Nuclei were visualized with the digital imaging system as described above.

Statistical analysis

The data were analyzed using one-way ANOVA analysis of variance, Bonferroni's post hoc multiple comparison test. Only values of $p < 0.05$ were considered significant.

Results

Table 1 shows the ATP levels of the 143B cells, control cybrids (HGA) and LHON cybrids (two clones for each mutation, obtained from independent LHON probands) cultured in glucose medium. All cell lines where found to have a similar ATP content, ranging from 15 to 25 nmol/mg protein. The RJ206 cybrid cell line exhibited lower ATP values than controls, but the difference was not statistically significant. Indeed, we found no statistical difference also between the pooled values of the cybrids harboring the same LHON mutations as compared to the control cybrids (Table 1).

Table 1. ATP levels in 143B cells, control and LHON cybrids incubated in glucose- containing medium.

Mutation	Clones	nmol/mg protein*	nmol/mg protein**
–	143B	24.4 ± 4.2 (8)	
–	HGA	23.7 ± 2.2 (6)	
11778	HFF	18.8 ± 1.7 (4)	21.7 ± 4.1
	HPE	23.5 ± 6.7 (5)	
3460	HMM	19.7 ± 5.0 (5)	17.4 ± 3.0
	RJ206	14.7 ± 2.4 (4)	
14484	HBA	18.7 ± 5.0 (5)	22.0 ± 4.5
	HL180	25.2 ± 7.7 (5)	

Description and origin of cell lines is detailed in ref.[8] Cells were seeded in 6 well plates, incubated for 24 h in DMEM-glucose medium and ATP content determined, as described in Material and methods.
*Data are means ± SEM, with number of experiments in parenthesis. Each experiment was carried out in duplicate.
**Data (means ± SD) were pooled for each LHON mutation.

By replacing glucose with galactose in the medium, the ATP levels did not significantly change up to 6h and only slightly decreased (approx. 30%) after 16h in control cybrids, whereas an increase was noted in 143B cells (Figure 1A). Conversely, the time-course of ATP level changes in LHON cybrids, illustrated in Figure 1B-D, showed that after 3-6h incubation in galactose medium, cellular ATP was remarkably decreased in all clones. In particular, LHON cybrids carrying the 3460/ND1 and 14484/ND6 mutations exhibited a more drastic average reduction in ATP content than 11778/ND4 mutants (at 3h, average values obtained from two clones: 36%, 23%, 43%, respectively). After 16h incubation in galactose medium, the average amount of ATP was about 15% in cybrids harboring the 11778/ND4 mutation, and even less in the clones with the other two LHON mutations.

The activation of caspase-3 during incubation of LHON cybrids in galactose medium was then investigated. Caspase-3 activation was first assessed using the fluorescent substrate Ac-DEVD-AMC. Figure 2A shows the time-course of Ac-DEVD-AMC cleavage in 143B cells or in control (left panel) and two cybrid clones for each LHON mutation (right panel) incubated in galactose medium. No significant increase of DEVDase activity was observed. No cleavage of procaspase-3 was discovered by western blot analysis (Figure 2B, panel left), in agreement with previous reports.[9] As a positive control, LHON cybrids with the 11778/ND4, 14484/ND6 and 3460/ND1 mutations were incubated with staurosporine, a well-known inducer of apoptotic cell death that operates via a caspase-dependent mitochondrial pathway.[25,26] Incubation for 6 h in the presence of 1 μM staurosporine caused a significant activation of DEVDase activity (Figure 2A, left panel) and the cleavage of procaspase-3, generating the 20 kDa fragment, already apparent after 3h in HGA and LHON cybrids (Figure 2B, right panels). Cell lysates prepared from the 143B parental cell line, control (not shown) and LHON cybrids were also probed for DFF45, one of the targets of caspase-3.[13] The two very close bands detected in the blot did not change after incubation in galactose medium (Figure 2C, left panel), whereas the 45 kDa band disappeared after staurosporine treatment (Figure 2C, right panel). Cleavage by staurosporine indicates that this band corresponds to DFF45, which is not processed after galactose incubation. Finally, pre-treatment of LHON cybrids with the broad caspase inhibitor benzyloxycarbonyl-Val-Ala-Asp-fluoromethyl ketone (z-VAD-fmk, 100 μM) failed to increase the viability of cells incubated in galactose medium (Figure 3A). This Figure also shows that cybrids carrying the 3460/ND1 and 14484/ND6 mutations were more sensitive to metabolic stress than those carrying the 11778/ND4 mutation, in agreement with our previous study.[8] Conversely, preincubation of 143B cells, control cybrids (not shown) and LHON cybrids bearing

Figure 1. ATP levels of 143B cells, control and LHON cybrids incubated in galactose medium. 143B cells, control and LHON cybrids were incubated in DMEM-galactose medium for the times indicated, then scraped off the plate and ATP content determined as described in Materials and methods. (A) 143B cells and control cybrids (HGA). (B–D) Cybrids with the indicated LHON mutations. For each LHON mutations, two clones were analyzed. Data are expressed as % of ATP levels determined in glucose medium (time = 0). 100% values for each clone are reported in Table 1. Each data point is the mean ± SEM of at least three determinations. The asterisk (*) denotes values significantly different from untreated cells ($p < 0.05$).

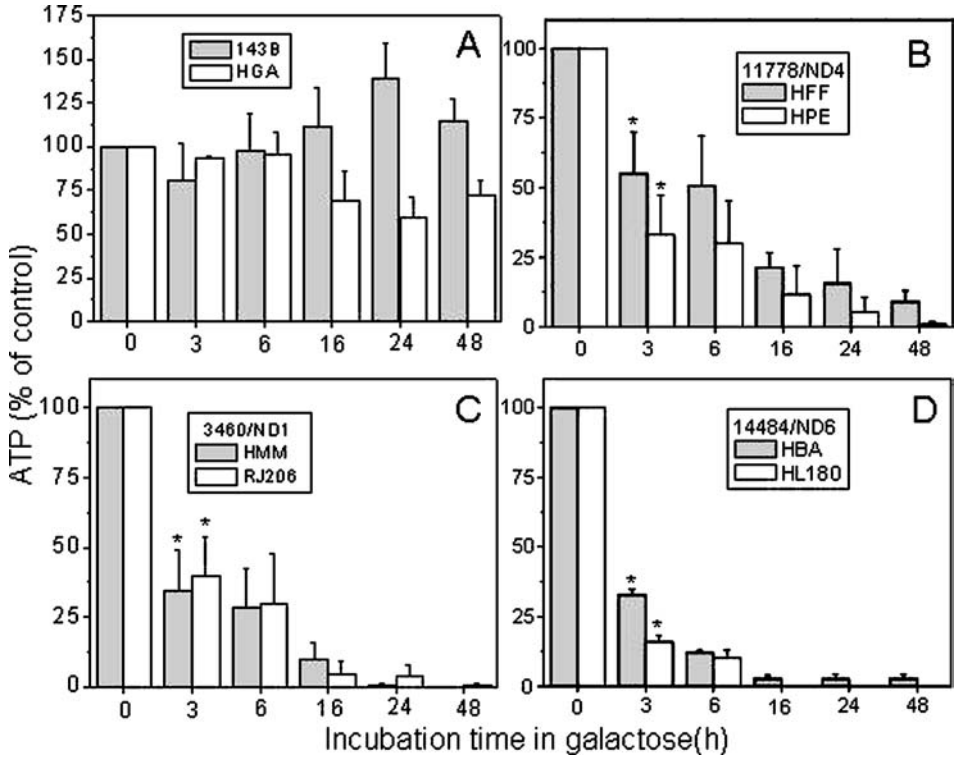

the 3460/ND1 mutation with z-VAD-fmk completely abolished the staurosporine-induced loss of cell viability (Figure 3B). Taken together, these results indicate that LHON cybrids can undergo caspase-independent cell death in galactose medium or caspase-mediated cell death in the presence of staurosporine.

We then decided to investigate the mechanism involved in the induction of nuclear oligonucleosomal DNA digestion or DNA laddering.[8] In several paradigms of apoptosis, lysosomes can function as death signal integrators, through the release of cathepsins into the cytosol.[28] The involvement of these proteases was ruled out by the finding that preincubation with pepstatin A (100 μM) or E-64-d (10 μM), specific inhibitors of cathepsin D and B, respectively, failed to protect LHON cybrids from death in galactose medium (result not shown).

We then focused our attention upon AIF and EndoG, which are known to induce DNA degradation through an essentially caspase-independent cell death mechanism.[15,18,19] The levels of these two mitochondrial apoptogenic factors and cytochrome c were first determined in the cytosolic fractions isolated from homogenates of cells incubated in galactose medium. Figure 4A shows that in control cybrids no mitochondrial apoptogenic factor was released from mitochondria during incubation in galactose medium. However, in cybrids with the 11778/ND4 mutation, and especially in those with the 3460/ND1 mutation, a weak but reproducible release of cytochrome c was detected after 16 and 6 h, respectively. AIF on the other hand was released after 24 and 16 h, respectively. Endo G levels did not change in the cytosolic fractions of control or LHON cybrids with the 11778/ND4 mutation, whereas in clones with the 3460/ND1 mutation, a weak amount was detected after 16 h followed by a more robust increase after 24 h. As a control, we also determined Endo G and AIF levels in the mitochondrial fractions. AIF levels did not change in control cybrids, but were significantly reduced after 24 h in cybrids with the 11778/ND4 mutation and already after 16 h in those with the 3460/ND1 (Figure 4B) and 14484/ND6 mutations (result not shown). A decrease of EndoG was apparent only after 48 h in cybrids carrying the 11778/ND4 mutation and after 16–24 h in those with the 3460/ND1 (Figure 4B) and 14484/ND6 mutations (result not shown).

Figure 2. Caspase-3 is not activated in LHON cybrids incubated in galactose medium. (A) 143B cells, control (HGA) (left panel) and LHON cybrids (two different clones for each LHON mutation, right panel) were incubated in DMEM-galactose medium for the times indicated or for 6 h in DMEM-glucose containing 1 μM staurosporine (STS). Caspase-3 activation was determined in cell lysates from the fluorescence of Ac-DEVD-AMC substrate developed in 1 h (ΔF), and is expressed as ratio of ΔF of cells incubated in galactose over ΔF of cells incubated in glucose. Data are means $\pm$ SD of at least three determinations. (B) Cells were incubated for the times indicated in DMEM-galactose (left panel) or in DMEM-glucose containing 1 μM staurosporine (STS, right panels). The levels of procaspase-3 in cell lysates were determined by Western blotting analysis, as described in Materials and methods. (C) Cells were incubated for the times indicated in DMEM-galactose (left panel) or in DMEM-glucose with 1 μM staurosporine (STS, right panel) and DFF45 cleavage determined by Western analysis. Tubulin was used as control for loading. Representative blots are shown.

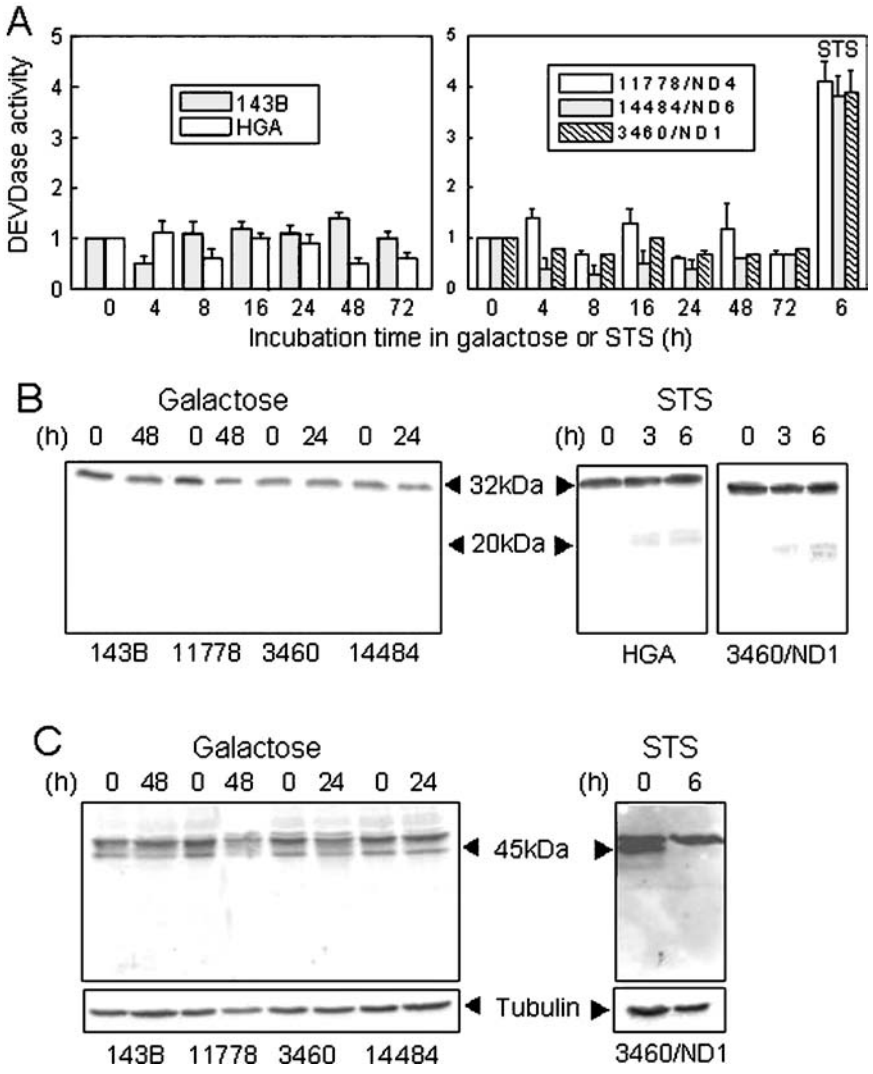

To confirm the western-blotting results, immunofluorescence analysis was used to determine the cellular localization of cytochrome c and EndoG during incubation of cybrids with the 14484/ND6 mutation in galactose medium. Unfortunately, we were unable to see any clear fluorescence signal from polyclonal anti-human AIF antibody. This was most likely due to the low level of expression of this protein in a single cell. After 16h incubation in galactose medium, most of the nuclei were still normal. The only condensed nucleus belonged to a cell exhibiting diffuse cytochrome c, but EndoG was retained within mitochondria (Figure 5A, upper panels). After 24 h incubation, the percentage of cells with fragmented nuclei increased (45 ± 8, $n = 5$). Most of the cells with condensed nuclei exhibited diffuse cytochrome c and EndoG staining (Figure 5A, lower panels). Together the results of Figs. 4 and 5A clearly indicate that cytochrome c, AIF and EndoG are released by mitochondria at different times during incubation of LHON cybrids in galactose medium.

Lastly, to determine whether AIF and EndoG are required for induction of the caspase-independent nuclear

Figure 3. Effect of the caspase inhibitor z-VAD-fmk on viability of LHON cybrids incubated in galactose medium or treated with staurosporine. Cybrids with the indicated LHON mutations were incubated for 24 h in DMEM-galactose medium (A) or in DMEM-glucose medium containing 1 μM staurosporine (B), in the absence or presence of 100 μM z-VAD-fmk. Cell viability was assessed with the MTT assay. Data are means $\pm$ SD of at least 3 determinations.

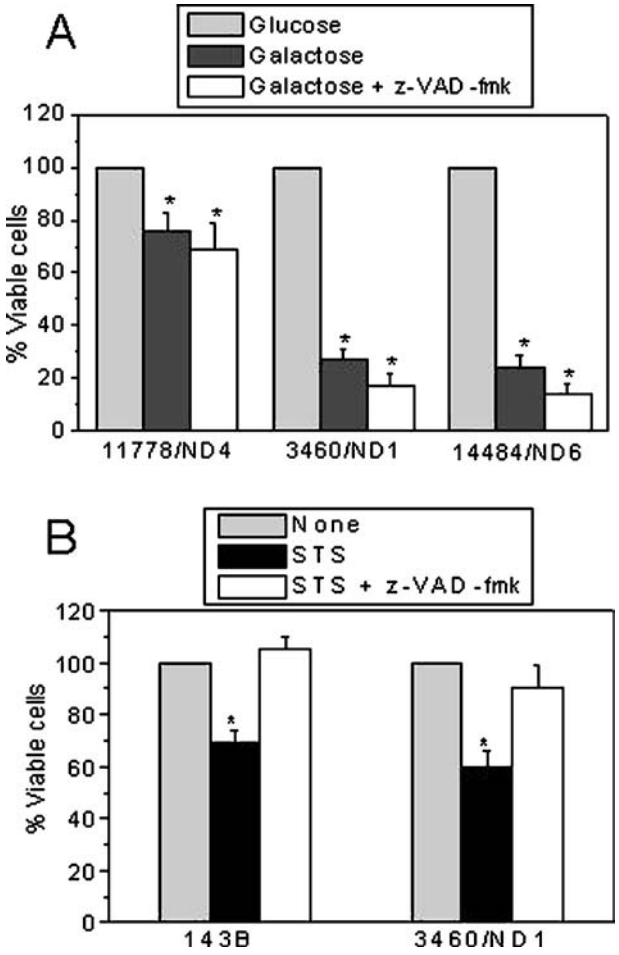

changes, we utilized a cell-free assay for nuclear fragmentation. Nuclei isolated from HeLa cells were incubated in cytosolic extracts derived from LHON cybrids grown in glucose or incubated for 24 h in galactose medium. Nuclei were visualized using Hoechst staining. Whereas the nuclear morphology was normal after incubation with glucose extracts (Figure 5B, panel a), galactose extracts induced the typical fragmentation of most nuclei (Figure 5B, panel b). However, when an aliquot of the same cytosolic extract obtained from cybrids maintained in galactose medium was immunodepleted of AIF and EndoG by 2 h treatment with the relevant antibodies, the number of nuclei with a fragmented morphology significantly decreased (65 $\pm$ 12%, $n = 4$ and 20 $\pm$ 10, $n = 4$, without or with immunodepletion, respectively; nuclei shown in Figure 5B, panel c). These results

Figure 4. Cytochrome c, AIF and EndoG levels in cytosolic and mitochondrial fractions isolated from control and LHON cybrids incubated in galactose medium. Control (HGA) and LHON cybrids were incubated in DMEM-galactose medium for the times indicated, then harvested and cytosolic and mitochondrial fractions were isolated, as described in Materials and methods. 50–80 μg of cytosolic (A) or mitochondrial (B) fractions were separated by SDS-PAGE and Western blotting was performed with specific antibodies. As control for loading, actin and mitochondrial heat shock protein-70 (mtHsp70) were used in the cytosolic and mitochondrial fractions, respectively. Representative blots are shown.

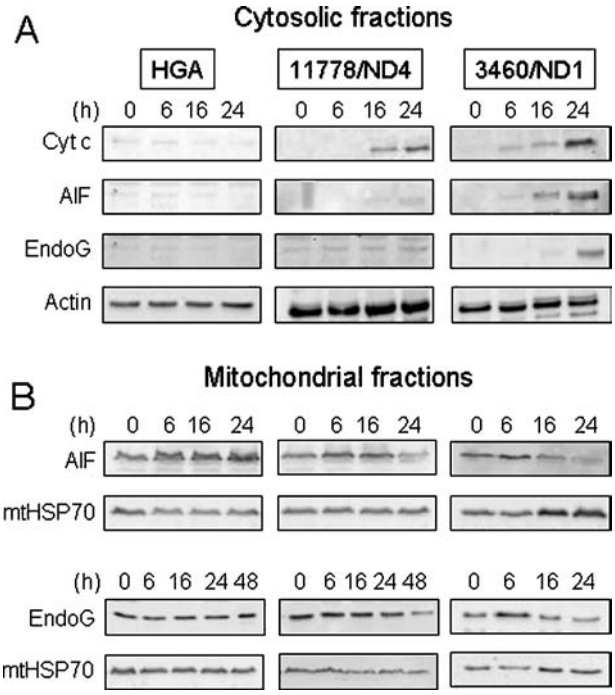

clearly indicate that AIF and EndoG are required for the induction of chromatin condensation.

Discussion

The current investigation into the apoptotic death pathway in LHON cybrids maintained in galactose medium allowed us to make the following conclusions. Firstly, cybrids bearing the three common LHON mtDNA mutations are consistently unable to maintain their ATP content during incubation in galactose medium. In addition, this energetic failure, which parallels the cybrid death curve, involves a caspase-independent pathway, which is mediated by AIF and EndoG.

The rapidly progressive ATP depletion was found to be a unique characteristic pertaining to the LHON cybrids, as control cybrids and 143B cells maintained their ATP content in galactose medium, being able to survive and even proliferate with this carbon source.[8] The ATP content of control and LHON cybrids is mostly generated by glycolysis. In fact, incubation of these cells in glucose

Figure 5. Immunofluorescence analysis of cytochrome c and EndoG release from mitochondria during incubation with galactose medium and *in vitro* assay for nuclear fragmentation. (A) 14484/ND6 LHON cybrids were incubated in DMEM-galactose medium for 16 and 24 h, fixed and stained with anti-cytochrome c or anti-EndoG primary antibody. Cytochrome c was visualized with FITC-secondary antibody and EndoG with TRITC- secondary antibody, as described in Material and methods. Nuclei were visualized after loading with 1 μg/ml Hoechst. Images were captured with a digital system under an inverted epifluorescence microscope. A representative experiment is shown. Arrows indicate apoptotic cells. Scale bars, 15 μm. (B) Nuclei isolated from HeLa cells were incubated in cytosolic extracts isolated from 14484/ND6 LHON cybrids in DMEM-glucose medium (panel a) or incubated for 24 h in DMEM- galactose medium (panel b). An aliquot of cytosolic extract obtained from cells incubated in galactose medium was then immunoprecipitated with anti-AIF and anti-EndoG antibodies (panel c). Nuclei were visualized after loading with 1 μg/ml Hoechst. Images was captured with a digital system under an inverted epifluorescence microscope with Plan-Apo 63X/1.4 oil objective. A representative experiment is shown. Scale bars, 15 μm.

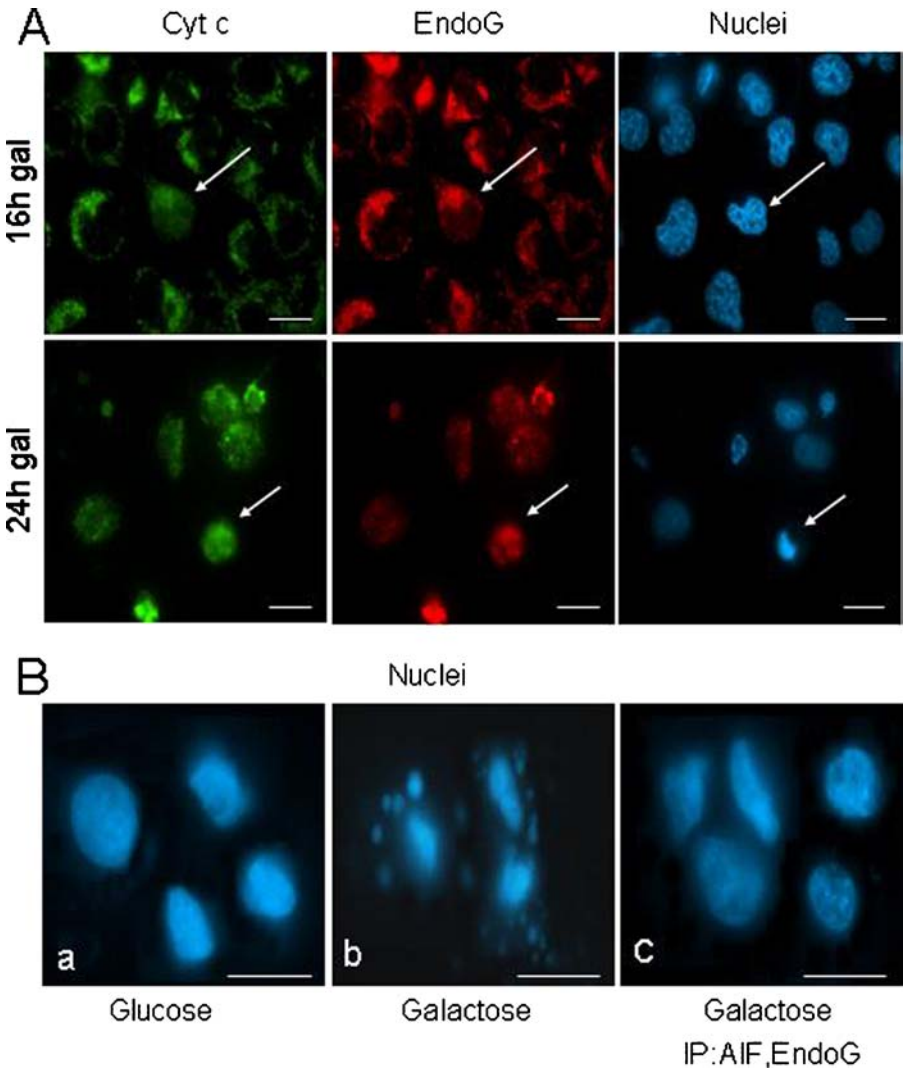

medium in the presence of rotenone or oligomycin or both these inhibitors did not significantly reduce their ATP content (our unpublished result). These results are in agreement with recent data showing that cybrids with severely defective oxidative phosphorylation, such as those carrying the neuropathy, ataxia, and retinitis pigmentosa (NARP) or mitochondrial encephalomyopathy, lactic acidosis and stroke-like episodes (MELAS) mtDNA mutations, maintained a normal ATP content in glucose medium, also in the presence of oligomycin.[29] It is therefore likely that, in glucose medium, glycolytically generated ATP is utilized to maintain the mitochondrial membrane potential ($\Delta\Psi_m$). Thus, the drastic reduction of glycolytic flux, caused by substitution of galactose for glucose in the medium, would force cells to derive ATP from mitochondrial oxidation of pyruvate.[30] Despite the fact that the respiration of LHON cybrids bearing 11778/ND4 mutation was previously reported as normal, the rate of ATP synthesis in digitonin-permeabilized cybrids was reduced by 60% when driven by complex I substrates.[22,23]

Thus, it is likely that the energetic failure, which is compensated *in vivo* under glycolytic conditions, only becomes relevant under the stressful conditions imposed by the galactose model and may play an unpredicted role in LHON pathophysiology.

In fact, the current study indicates that the energetic failure of LHON cybrids in galactose medium shaped the pathway of cell death. We clearly show that despite the significant release of cytochrome c from mitochondria, the death process was caspase-independent. Given that both cytochrome c and ATP are required for the assembly of the apoptosome and subsequent caspase-9 activation, the early drastic reduction of ATP levels is likely to impair the formation of the oligomeric complex and consequently abort the activation of the caspases cascade.[31] A significant stimulation of caspase-3 cleavage was previously reported in the same LHON cybrid cell lines treated with anti-Fas antibody.[6] We have also shown here that caspase-3 can be activated after treatment with staurosporine. Although the involvement of other caspases cannot be completely ruled out, it is noteworthy that, in addition to caspase-3, caspase-6, -7, -8 and -10 may also have some affinity to cleave the Ac-DEVD-AMC oligopeptide. Therefore the lack of DEVD and DFF45 cleavage, in conjunction with the inability of the pan caspase inhibitor z-VAD-fmk to promote cell survival, strongly suggests that these executioner caspases are not activated during LHON cybrids death in the galactose model.

The presence of nuclear fragmentation in the absence of caspase activation raised the possibility that other pathways of cell death may be in play.[14] Indeed we documented that, in addition to cytochrome c, AIF and EndoG are also released from mitochondria into the cytosol during cell death of LHON cybrids in galactose medium. The inhibition of nuclear fragmentation obtained in the cell-free assay after immunodepletion of these apoptogenic factors strongly indicates that AIF and Endo G are required for nuclear chromatin fragmentation and the oligonucleosomal DNA degradation previously reported.[8] The hierarchy of mitochondrial apoptogenic factor release is controversial and usually studied in cell models with caspase activation inhibited by z-VAD-fmk.[16,32,33] In the galactose model of LHON cybrid death here reported, which occurs in the absence of any significant caspase activation, we observed by western blot analysis of cytosolic and mitochondrial fractions and by immunofluorescence studies, that cytochrome c release preceded that of AIF, which was followed by EndoG. These findings are in accordance with recent data showing that AIF is peripherally associated with mitochondrial inner membrane, while EndoG may be located in the matrix, or tightly bound to the inner membrane.[16] In the caspase-independent camptothecin-induced neuronal cell death, cytochrome c release was also shown to precede AIF translocation.[33] However, in cells treated with Bax/Bak-dependent pro-apoptotic drugs, the release of AIF and EndoG, but not of cytochrome c, was prevented by the caspase inhibitor z-VAD-fmk, suggesting that a caspase-dependent step is required.[16,34] It is likely that the sequence of mitochondrial events may depend on the cell type and/or mode of apoptotic induction. Furthermore, other factors might influence the rate of release of apoptogenic factors, altering the mode and extent of mitochondrial permeabilization.[32,34]

Conclusion

In conclusion, we propose that during the galactose-induced death of LHON cybrids, the early reduction of ATP levels prevents the onset of the "classical" cytochrome c-mediated caspase-dependent pathway. However, the release of AIF and EndoG from mitochondria into the cytosol, and their subsequent translocation into the nucleus can account for the typical changes in chromatin structure and completion of the cell death process. On the other hand, the presence of some typical apoptotic hallmarks[8] when the ATP levels are reduced below the values critical for the caspase-dependent execution of the apoptotic process, estimated at 25% of the normal ATP value,[35] suggests that the cell death mediated by AIF and Endo G can proceed also under a rather impaired energetic status. It must be noted that under these conditions the percentage of necrotic cells, determined by acridine orange/ethidium bromide loading, was previously reported to be negligible.[8]

The LHON cybrid galactose model has proven very helpful to investigate cell death pathways in relation to the pathogenic mtDNA mutations. We are aware that the drastic conditions established with this model are artificially set and not necessarily match what may occur *in vivo*.[26] However, a number of conditions such as environmental toxins, in particular tobacco smoking,[36] and nuclear genetic factors determining, for instance, less efficient antioxidant mitochondrial machinery,[37] may tip RGC over a threshold leading to bioenergetic failure and rapid ATP depletion. This may play a role in driving cellular death following a pattern similar to that observed in our galactose model of LHON cybrids.

The RGC system is believed to be particularly sensitive to both energy production and mitochondrial distribution.[4] This is due to the skewed functional properties of the RGC derived axons, which run unmyelinated in the nerve fibre layer of the retina, and after turning into the optic nerve head, acquire the myelin sheath having passed the lamina cribrosa. The myelinated postlaminar portion of the optic nerve is less energy dependent compared to the more anterior unmyelinated portion, because of the saltatory conduction of action potentials. Thus, mitochondria are concentrated within the initial unmyelinated stretch of the RGC axons where energy is needed to maintain

the ion pumping for an efficient transmission of action potentials.[4] The role of ATP availability in such a system may be of great importance in LHON pathophysiology. In this regard, it is becoming clear that at least some of the cell death pathways in chronic neurodegenerative diseases follow mechanisms alternative to those mediated by caspases.[14] Further studies, possibly taking advantage of animal models,[38,39] or by using cells derived from patients (*i.e.* fibroblasts) are needed to establish the exact sequence of events at the molecular and cellular level in the target tissue. However, we believe that our experimental model could be useful to study therapeutic strategies aimed at preventing or at least limiting the activation of apoptotic cellular death.

Acknowledgments

We thank Dr. D.X. Wang, USA, for the gift of anti-EndoG antibodies, Dr. A.H.V. Schapira, UK, for providing the RJ206 cells and Dr. D. Arnoult, France, for helpful comments. This work was supported by grants from Telethon Italy no.GGP02323 (to VC) and from MIUR (to MR). CZ was supported by Telethon funding.

References

1. Newman NJ. Leber's optic neuropathy. In: Miller NR, Newman NJ, eds. *Walsh and Hoyt's Clinical Neuro-Ophthalmology*. Baltimore: Williams & Wilkins 1998: 742–753.
2. Carelli V. Leber's hereditary optic neuropathy. In: Schapira AHV and Di Mauro S eds, 2nd *Mitochondrial Disorders in Neurology* 2. Boston: Butterworth-Heinemann Blue Books of Practical Neurology 2002: 115–142.
3. Brown MD. The enigmatic relationship between mitochondrial dysfunction and Leber's hereditary optic neuropathy. *J Neurol Sci* 1999; **165**: 1–5.
4. Carelli V, Ross-Cisneros FN, Sadun AA. Mitochondrial dysfunction as a cause of optic neuropathies. *Prog Retin Eye Res* 2004; **23**: 53–89.
5. King MP, Attardi G. Isolation of human cell lines lacking mitochondrial DNA. *Methods Enzymol* 1996; **264**: 304–313.
6. Danielson SR, Wong A, Carelli V, Martinuzzi A, Schapira AHV, Cortopassi AG. Cells bearing mutations causing Leber's hereditary optic neuropathy are sensitized to Fas-Induced apoptosis. *J Biol Chem* 2002; **277**: 5810–5815.
7. Robinson BH, Petrova-Benedict R, Buncic JR, Wallace DC. Nonviability of cells with oxidative defects in galactose medium: A screening test for affected patient fibroblasts. *Biochem Med Metab Biol* 1992; **48**: 122–126.
8. Ghelli A, Zanna C, Porcelli AM, *et al*. Leber's hereditary optic neuropathy (LHON) pathogenic mutations induce mitochondrial-dependent apoptotic death in transmitochondrial cells incubated with galactose medium. *J Biol Chem* 2003; **278**: 4145–4150.
9. Zanna C, Ghelli A, Porcelli AM, Carelli V, Martinuzzi A, Rugolo M. Apoptotic cell death of cybrids bearing LHON mutations is caspase-independent. *Ann NY Acad Sci* 2003; **1010**: 213–217.
10. Zou H, Henzel WJ, LiuX, Lutschg A, Wang XD. Apaf-1, a human protein homologous to C. elegans CED-4, participates in cytochrome c-dependent activation of caspase-3. *Cell* 1997; **90**: 405–413.
11. Li P, Nijhawan D, Budihardjo I, *et al*. Cytochrome c and dATP-dependent formation of Apaf-1/caspase-9 complex initiates an apoptotic protease cascade. *Cell* 1997; **91**: 479–489.
12. Enari M, Sakahira H, Yokoyama H, Okawa K, Iwamatsu A, Nagata S. A caspase-activated DNase that degrades DNA during apoptosis, and its inhibitor ICAD. *Nature* 1998; **391**: 43–50.
13. Liu X, Li P, Widlak P, Zou H, Garrard WT, Wang X. The 40-kDa subunit of DNA fragmentation factor induces DNA fragmentation and chromatin condensation during apoptosis. *Proc Natl Acad Sci USA* 1998; **95**: 8461–8466.
14. Leist M and Jäättelä M. Four deaths and a funeral: From caspases to alternative mechanisms. *Nature Rev Mol Cell Biol* 2001; **2**: 1–10.
15. Susin SA, Lorenzo HK, Zamzami N, *et al*. Molecular characterization of mitochondrial apoptosis-inducing factor. *Nature* 1999; **397**: 441–446.
16. Arnoult D, Gaume B, Karbowski M, Sharpe JC, Cecconi F, Youle RJ. Mitochondrial release of AIF and EndoG requires caspase activation downstream of Bax/Bak-mediated permeabilization. *EMBO J* 2003; **22**: 4385–4399.
17. Vahsen N, Cande C, Briere JJ, *et al*. AIF deficiency compromises oxidative phosphorylation. *EMBO J* 2004; **23**: 4679–2689.
18. Lorenzo HK, Susin SA. Mitochondrial effectors in caspase-independent cell death. *FEBS Lett* 2004; **557**: 14–20.
19. Li LY, Luo X, Wang X. Endonuclease G is an apoptotic DNase when released from mitochondria. *Nature* 2001; **412**: 95–99.
20. Widlak P, Li LY, Wang X, Garrard WT. Action of recombinant human apoptotic endonuclease G on naked DNA and chromatin substrates: Cooperation with exonuclease and DNase I. *J Biol Chem* 2001; **276**: 48404–48409.
21. Wang X, Yang C, Chai J, Shi JY, Xue D. Mechanisms of AIF-Mediated Apoptotic DNA Degradation in *Caenorhabditis elegans*. *Science* 2002; **298**: 1577–1592.
22. Guy J, Qi X, Pallotti F, *et al*. Rescue of a mitochondrial deficiency causing Leber Hereditary Optic Neuropathy. *Ann Neurol* 2002; **52**: 534–542.
23. Baracca A, Solaini, Sgarbi G, *et al*. Severe impairment of complex I-driven ATP synthesis in Leber's hereditary optic neuropathy. *Arch Neurol* 2005; **62**: 730–736.
24. Bradford MM. A rapid and sensitive method for the quantitation of microgram quantities of protein utilizing the principle of protein-dye binding. *Anal Biochem* 1976; **72**: 248–254.
25. Ghelli A, Porcelli AM, Zanna C, Rugolo M. 7-Ketocholesterol and staurosporine induce opposite changes in intracellular pH, associated with distinct types of cell death in ECV304 cells. *Arch Biochem Biophys* 2002; **402**: 208–217.
26. Porcelli AM, Ghelli A, Zanna C, Valente P, Ferroni S, Rugolo M. Apoptosis induced by staurosporine in ECV304 cells requires cell shrinkage and up-regulation of Cl^- conductance. *Cell Death Differ* 2004; **11**: 665–672.
27. Martin SJ, Green DR. Cell-free apoptosis. In: Cotter TG and Martin SJ Eds. Techniques in Apoptosis. Portland: Press Ltd. London UK 1996: 121–132.
28. Jäätela M, Cande C and Kroemer G. Lysosomes and mitochondria in the commitment to apoptosis: A potential role for cathepsin D and AIF. *Cell Death Differ* 2004; **11**: 135–136.
29. Gajewski CD, Yang L, Schon EA, Manfredi G. New insights into the bioenergetics of mitochondrial disorders using intracellular ATP reporters. *Mol Biol Cell* 2003; **14**: 3628–3635.

30. Robinson BH. Use of fibroblast and lymphoblast cultures for detection of respiratory chain defects. *Methods Enzymol* 1996; **264**: 454–464.
31. Nicotera P. Apoptosis and age-ralated disorders: Role of caspase-dependent and caspase-independent pathways. *Toxicol Lett* 2002; **127**: 189–195.
32. Cregan SP, Dawson L, Slack RS. Role of AIF in the caspase-dependent and caspase-independent cell death. *Oncogene* 2004; **23**: 2785–279.
33. Cregan SP, Fortin A, McLaurin JG, *et al*. Apoptosis-Inducing Factor is involved in the regulation of caspase-independent neuronal cell death. *J Cell Biol* 2002; **158**: 507–517.
34. Arnoult D, Karbowski M, Youle RJ. Caspase inhibition prevents the mitochondrial release of apoptosis-inducing factor. *Cell Death Differ* 2003; **10**: 845–849.
35. Leist M, Single B, Castoldi AF, Kuhnle S, Nicotera P. Intracellular adenosine triphosphate (ATP) concentration: A switch in the decision between apoptosis and necrosis. *J Exp Med* 1997; **185**: 1481–1486.
36. Sadun AA, Carelli V, Salomao SR, *et al*. Extensive investigation of a large Brazilian pedigree of 11778/haplogroup J Leber hereditary optic neuropathy. *Am J Ophthalmol* 2003; **136**: 231–238.
37. Carelli V, Giordano C, D'Amati G. Pathogenic expression of homoplasmic mtDNA mutations needs a complex nuclear-mitochondrial interaction. *Trends Genet* 2003; **19**: 257–262.
38. Qi X, Lewin AS, Hauswirth WW, Guy J. Optic neuropathy induced by reductions in mitochondrial superoxide dismutase. *Invest Ophthalmol Vis Sci* 2003; **44**: 1088–1096.
39. Qi X, Lewin AS, Hauswirth WW, Guy J. Suppression of complex I gene expression induces optic neuropathy. *Ann Neurol* 2003; **53**: 198–205.